

The solar cycle: parity interactions and amplitude modulation

S.M. Tobias*

Department of Applied Mathematics and Theoretical Physics, University of Cambridge, Cambridge CB3 9EW, UK

Received 12 November 1996 / Accepted 6 December 1996

Abstract. Two mechanisms for producing modulation of the basic eleven year solar cycle are included in a nonlinear $\alpha\omega$ dynamo model. In the first, the modulation of the toroidal magnetic field energy is associated with large changes in the parity (symmetry) of solutions. The second mechanism introduces modulation of the magnetic field by including the action of the Lorentz force in driving macrodynamic velocity perturbations (the Malkus-Proctor mechanism) in the limit of small magnetic Prandtl numbers. The nonlinear model shows that solutions can display both types of modulation in different parameter regimes. For a suitable choice of parameters solutions display behaviour similar to that observed on the Sun. The magnetic field is significantly modulated whilst staying largely dipolar. However when the field is weak, during Grand Minima, the field is no longer symmetric and magnetic activity is confined to one hemisphere.

Key words: MHD – Sun: magnetic fields; activity

1. Introduction

Sunspots, which are surface manifestations of the Sun's toroidal magnetic field, appear at mid-latitudes and migrate towards the equator. The polarity of the spots is different in each hemisphere (Hale's polarity law) and reverses with an average period of eleven years. This basic twenty-two year solar magnetic cycle is modulated on a longer time-scale of approximately 80–90 years. The modulation takes the form of more (respectively fewer) spots initially appearing at higher (respectively lower) latitudes. The modulation is easily seen in record of sunspot numbers (an arbitrary measure of solar magnetic activity). These records (e.g. Eddy 1976) also indicate that during the 17th century solar activity died out almost completely. Very few sunspots were observed although strenuous observations were being undertaken at that time in Paris (see Ribes & Nesme-Ribes 1993) and by Flamsteed, the Astronomer Royal in England (Hoyt & Schatten 1995). Moreover observations of sunspots in the late seventeenth century also indicate that the solar magnetic activity was asymmetric as the Sun emerged from the Maunder minimum, with sunspots only appearing in the northern solar

hemisphere for a couple of solar cycles (Sokoloff & Nesme-Ribes 1994). After these two cycles the Sun appeared to regain its dipolar symmetry and Hale's polarity laws were largely obeyed (Watari 1996). Proxy data, for example terrestrial ^{14}C and ^{10}Be records (Stuiver et al. 1995; Beer et al. 1991) demonstrate that the Maunder minimum is not an isolated event and that solar activity is recurrently interrupted by Grand Minima on a time-scale of approximately 200 years.

The accepted explanation of solar activity is that the magnetic field is generated by a magneto-hydrodynamic dynamo acting at the base of the convection zone. Most solar dynamo calculations employ the mean field electrodynamics (MFE) approximation to derive the $(\alpha\omega)$ dynamo equations from the induction equation. In this approximation the magnetic field is split into its mean and fluctuating parts, and an equation for the large-scale (mean) magnetic field is derived by making certain assumptions about the form of the correlations between the small-scale magnetic field and the turbulent velocity field.

Many mean-field dynamo models are capable of replicating modulation of the basic magnetic cycle (e.g. Brandenburg et al. 1989; Kitchatinov et al. 1994) so that the magnetic energy of solutions undergoes periods of reduced activity. However in these models the parity of solutions (an analogue of the symmetry of the butterfly diagram) varies considerably as the solution is modulated. We will henceforth refer to this type of modulation of the basic cycle as Type 1 modulation. As noted earlier, this is not the behaviour observed on the Sun, where significant changes in the magnetic energy are possible without large fluctuations in parity, except when a minimum energy state is entered and the parity may change significantly.

In an attempt to understand the nonlinear processes that may lead to modulation of the solar cycle, much attention has focussed on simple models. Low-order models may be derived by truncating Galerkin expansions in the dynamo equations (e.g. Weiss et al. 1984). These models naturally yield solutions where the basic cycle is significantly modulated, but are open to the criticism that any behaviour found may be an artifact of the truncation and not an inherent property of the full system. Another approach is to study the dynamics of simple systems that naturally exhibit bursts of activity interspersed with quiescent periods (Platt et al. 1994). Studying this 'on-off intermittency' in simple systems leads to a greater understanding of the dif-

* *Present address:* Joint Institute for Laboratory Astrophysics, Boulder, Colorado, CO 80309-0440 USA

ferent ways in which the solar cycle may emerge from minima. In order to characterize the Type 1 modulation, Knobloch & Landsberg (1996) derived a set of model equations that could successfully describe the parity interactions found in the models discussed earlier. They show that modulation of the basic cycle follows as a direct consequence of including the interaction of modes with the appropriate symmetries. A different mechanism for modulation was considered by Tobias et al. (1995), who derived a simple third order model and ascribed the modulation to changes in the large-scale velocity of the Sun. They relied on the power of normal-form-theory to ensure that the results were robust. As in the truncated model of Weiss et al. (1984) chaotically modulated solutions followed a series of Hopf bifurcations and the breakdown of a torus to form a chaotic attractor.

The success of this toy-model was demonstrated when the behaviour found for the simplified equations were reproduced in the untruncated PDEs (Tobias 1996a). In that paper significant modulation of the basic magnetic cycle was obtained by considering a more sophisticated (and more natural) nonlinearity than the simple quenching mechanisms that had largely been included in dynamo calculations. The ‘Malkus-Proctor effect’ (after Malkus & Proctor 1975) includes directly the effect of the large-scale magnetic field in driving velocity perturbations (the so-called torsional oscillations) via the Lorentz force. It was demonstrated that if a sufficiently small magnetic Prandtl number was considered then clear modulation of the basic magnetic cycle (and the occurrence of minima) could be found in a model where the dipole symmetry of solutions was imposed and the parity of solutions was fixed. This model however prescribed the symmetry of solutions and it is unclear whether the pure dipoles considered are the preferred solutions if the parity is free to evolve in the full problem. Moreover the model clearly precluded the possibility of solutions losing dipole symmetry when the field is low (as observed when the Sun emerged from the Maunder minimum).

This paper introduces a model where both potential modulational processes are considered. The Malkus-Proctor effect can lead to solutions where the modulational timescale (T_m) is controlled by the magnetic Prandtl number τ (which we shall call Type 2 modulation). Moreover no parity condition is imposed at the solar equator and so the solutions are free to modulate the energy by moving between solutions of different parity (Type 1 modulation). The results show that parameter regimes can be found where either type of modulation is dominant. For small dynamo numbers the Type 1 modulation appears to be more important, but as the dynamo number is increased the Type 2 modulation takes over and solutions can be found that exhibit large changes in magnetic energy with no change in symmetry. For large enough dynamo numbers solutions can be found that mimic the behaviour found on the Sun – i.e. they are modulated significantly and stay largely dipolar except when the field is weak when they may become asymmetric. This is the first non-linear $\alpha\omega$ dynamo model for which such solutions are found.

In the next section the model is derived and the differences from the model of Tobias (1996a) are discussed. The results are

described in Sects. 3 and 4 and the implications for describing the solar cycle are discussed in Sect. 5.

2. Derivation of the model

The model considered here is similar to that discussed in Tobias (1996a) except that solutions are sought in both the northern and southern hemisphere and no parity constraints are imposed at the equator. Solutions to the mean-field dynamo equation

$$\frac{\partial \mathbf{B}}{\partial t} = \nabla \times (\mathbf{v} \times \mathbf{B} + \alpha \mathbf{B} - \eta \nabla \times \mathbf{B}), \quad (1)$$

where \mathbf{v} is the large scale velocity field, are sought in a two-dimensional cartesian dynamo model. The spherical shell at the base of the solar convection zone hemisphere is modelled by a thin cartesian band $0 < x < 2L$, $-1 < z < 1$.

The axisymmetric mean magnetic field is decomposed into toroidal and poloidal parts,

$$\mathbf{B}(x, z) = B \hat{\mathbf{y}} + \nabla \times \mathbf{A} \hat{\mathbf{y}}.$$

We consider a large-scale toroidal velocity field of the form

$$\mathbf{v} = u(z) \sin(\pi x/2L) \hat{\mathbf{y}} + v(x, z) \hat{\mathbf{y}},$$

where the first term, $u(z) \sin(\pi x/2L) \hat{\mathbf{y}}$, corresponds to the large-scale radial shear ($G(z) = du/dz$) determined by helioseismology (see e.g. Thompson et al. 1996) to exist at the base of the solar convection zone (the ω -effect), and the latitudinal dependence on x sets the ω -effect to zero at the pole (cf. Jennings & Weiss 1991). The second term is the macrodynamic toroidal velocity driven by the large-scale Lorentz force (the ‘Malkus-Proctor effect’). It should be noted at this point that if the dynamo acts throughout the convection zone, then this effect may be of secondary importance to the modification of the angular momentum profile by the magnetic stress tensor (Λ -quenching) as argued by Kitchatinov et al. (1994). However in an overshoot model, where the strong magnetic field is stored in a thin layer away from the bulk of the turbulent convection, it is natural to consider the Malkus-Proctor effect as the non-linearity of greatest importance. The α -effect, which depends on Coriolis forces, should be antisymmetric about the equator and for simplicity we consider $\alpha = \alpha_0 f(z) \cos(\pi x/2L)$. The momentum equation for the mean velocity field \mathbf{v} is then given by

$$\rho \left(\frac{\partial \mathbf{v}}{\partial t} + (\mathbf{v} \cdot \nabla) \mathbf{v} \right) = -\nabla p + \nabla \cdot \sigma + 2\Omega \times \mathbf{v} + \mathbf{j} \times \mathbf{B} + \nabla \cdot \mathcal{F}, \quad (2)$$

where ρ is the density, p is the pressure, Ω is the rotation of the star, σ_{ij} is the stress tensor and \mathbf{j} is the large-scale current given by

$$\mathbf{j} = \frac{1}{\mu_0} \nabla \times \mathbf{B}.$$

The effects of rotation and magnetic field on the velocity are explicit in equation (2), and the other forces (e.g. gravity, thermal

forcing, Reynolds stresses from the small-scale turbulence) are contained in the tensor \mathcal{F} . In the calculations that follow, the vertical extent of the layer is considered to be small compared to a density scale height, and therefore the density ρ is set to a constant.

The decompositions for the magnetic field and velocity field are substituted into equations (1) and (2) to yield equations for the toroidal field (B), the vector potential for the poloidal field (A) and the velocity perturbations driven by the Malkus-Proctor effect (v). It is also possible to derive an equation that must be satisfied by the imposed shear $u(z) \sin(\pi x/2L) \hat{y}$. In this paper it is assumed that the shear has the imposed form given below, which is mathematically equivalent to stating that a forcing tensor \mathcal{F} can be found that drives the required velocity field.

The equations are then non-dimensionalised by setting

$$\begin{aligned} \mathbf{x} &= l \hat{\mathbf{x}}, & t &= l^2/\eta_0 \hat{t}, & \eta &= \eta_0 h, & \nu &= \nu_0 h, \\ \alpha &= \alpha_0 f(x, z), & G(z) &= \omega_0 g(z), & v(z) &= l\omega_0 \hat{v}(z), \\ A(z) &= lB_0\alpha_0 \hat{A}(x, z), & B(x, z) &= B_0 \hat{B}(x, z), \end{aligned}$$

where l is a characteristic length-scale in the z -direction. The non-dimensional equations are now (for constant ν and η in the $\alpha\omega$ -limit)

$$\begin{aligned} \frac{\partial A}{\partial t} &= h \nabla_H^2 A + f(z) \cos\left(\frac{\pi x}{2L}\right) B, \\ \frac{\partial B}{\partial t} &= h \nabla_H^2 B + D \left(g(z) \sin\left(\frac{\pi x}{2L}\right) + \frac{\partial v}{\partial z} \right) \frac{\partial A}{\partial x} \\ &\quad - D \left(\frac{\pi}{2L} u \cos\left(\frac{\pi x}{2L}\right) + \frac{\partial v}{\partial x} \right) \frac{\partial A}{\partial z}, \\ \frac{\partial v}{\partial t} &= \tau h \left[\frac{\partial^2 v}{\partial x^2} + \frac{\partial^2 v}{\partial z^2} \right] + R_\alpha \Lambda \left[\frac{\partial B}{\partial z} \frac{\partial A}{\partial x} - \frac{\partial A}{\partial z} \frac{\partial B}{\partial x} \right], \end{aligned} \quad (2)$$

where $\nabla_H^2 = \partial^2/\partial x^2 + \partial^2/\partial z^2$.

The non-dimensional parameters are

$$D = \frac{\alpha_0 \omega_0 l^3}{\eta_0^2}, \quad R_\alpha = \frac{\alpha_0 L}{\eta_0}, \quad \Lambda = \frac{B_0^2}{\rho_0 \mu_0 \eta_0 \omega_0}, \quad \tau = \frac{\nu_0}{\eta_0}$$

where D is the dynamo number, R_α is the ‘ α -effect Reynolds number’, Λ is the (modified) Elsasser Number and τ is the magnetic Prandtl number which measures the ratio of the viscous to magnetic diffusion timescales. The product $R_\alpha \Lambda$ may be set to $\text{sgn}(D)$ as it is the parameter in front of the only nonlinearity in the problem.

The radial dependence of the α -effect and shear is chosen to be the same as in the model of Tobias (1996a). The profiles for the radial dependence of these quantities is shown in Fig. 1. These profiles are chosen so that the scenario is similar in design to the linear model discussed by Parker (1993). This model has a strong shear at the base of the convection zone, which creates toroidal field and the poloidal field is recreated by the helical turbulence in the convection zone itself. The model relies on the turbulent transport of magnetic field between the two zones, and it has been demonstrated (Tobias 1996b) that this scenario may arise as a result of the action of the magnetic field on the turbulent transport in the overshoot region. Here, however, the turbulent

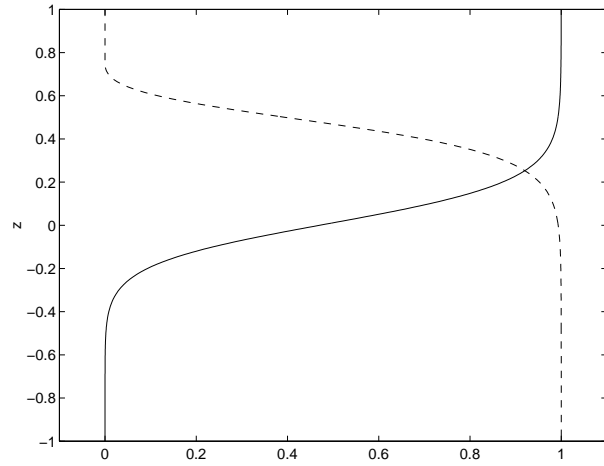


Fig. 1. The α effect (solid line) and shear (dashed line) as a function of depth (z): notice the region of overlap of the shear and α effect. The turbulent diffusivity is constant across the layer.

diffusion of both magnetic field and differential rotation are kept constant across the layer for numerical expediency, so ν and η are constant implying that $h = 1$.

The boundary conditions are set to be

$$\begin{aligned} A = B = v = 0 & \text{ at } x = 0, & A = B = v = 0 & \text{ at } x = 2L, \\ A = B = v = 0 & \text{ at } z = -1, & \partial_z A = B = \partial_z v = 0 & \text{ at } z = 1, \end{aligned}$$

so that solutions are free to select their own parity. In this way the possibility of obtaining symmetry-breaking bifurcations and parity modulation has been reintroduced into the model.

3. Results for fixed τ

In this section attention is restricted to the parameter regime $D < 0$, leading to the migration of magnetic activity towards the equator. It is a property of dynamo models where the α -effect is antisymmetric about the equator (Stix 1991) that the initial bifurcation to dynamo action must yield solutions of either pure dipole or quadrupole state. The critical dynamo numbers for solutions of these two symmetries are calculated by expanding the toroidal and poloidal magnetic fields, and solving the resulting two-point boundary value problem using the Newton-Raphson-Kantorovitch scheme NRK (see e.g. Gough et al. 1976). More details of this calculation can be found in the Appendix.

For comparison with the results in Tobias (1996a) the length from pole to equator is set to be $L=4$. The dipole mode is the first mode to become unstable at a Hopf bifurcation at $D = -279.32$. The eigensolution oscillates with a frequency $\omega = 5.22$. The quadrupole mode does not become unstable until $D = -324.75$ with a frequency of $\omega = 5.92$. Thus in the nonlinear calculations one would expect the dipole mode to be initially preferred.

The fully nonlinear problem is solved by time-stepping the equations using a mixed finite-difference pseudo-spectral discretisation of the equations together with a second order Adams-Bashforth time-stepping scheme. The latitudinal boundary con-

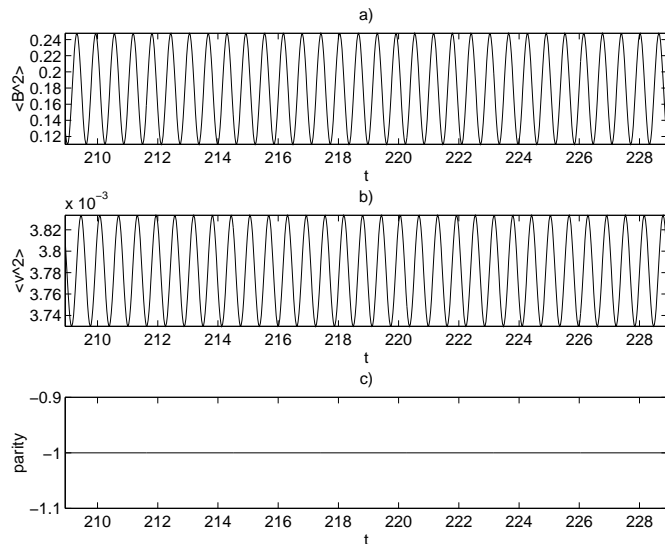


Fig. 2a–c. Oscillatory Dipole: $\tau = 0.1$, $D = -300$. **a** Periodic magnetic energy. **b** As for **a**, but time series of the average kinetic energy. **c** As for **b**, but time series is of the parity of solutions.

ditions are automatically satisfied by the spectral scheme which expands A , B and v as sine series.

In all cases useful diagnostics for analyzing the solutions are the magnetic energy $E = E_q + E_d$ and the parity of solutions (cf. Brandenburg et al. 1989),

$$P = \frac{E_q - E_d}{E_q + E_d},$$

where E_q and E_d are the total magnetic energy of the dipole and quadrupole modes respectively defined by

$$E_q = \int_{\mathcal{V}} \mathbf{B}_q^2 dV, \quad E_d = \int_{\mathcal{V}} \mathbf{B}_d^2 dV,$$

where \mathcal{V} is the domain of computation. Hence $P = -1$ corresponds to purely dipolar solutions whilst $P = 1$ is the pure quadrupole.

Here the magnetic Prandtl number τ is set to be as small as possible for the numerical scheme. Unfortunately, the minimum value of τ for which it was feasible to fully investigate the parameter regime is $\tau = 0.1$ (not the value $\tau = 0.01$ that was possible in the fixed parity case). Some selected calculations have been performed with a different value of τ and these will be presented in Sect. 4. As expected, an oscillatory dipole becomes unstable at a supercritical Hopf bifurcation as the dynamo number is decreased past the critical value $D = -279.32$. The time-series for the stable oscillatory dipole are shown in Fig. 2. In Fig. 2a the magnetic energy is shown to be oscillatory (with a period half that of the magnetic cycle) and Fig. 2b shows the overall kinetic energy in the velocity perturbations which is also periodic (with the same period as the magnetic energy). The parity is shown to be a constant $P = -1$ in Fig. 2c indicating that the solution is indeed dipolar.

The butterfly diagram (i.e. contour plot of the toroidal magnetic field B at a given level $z = 0.5$ versus time) is shown

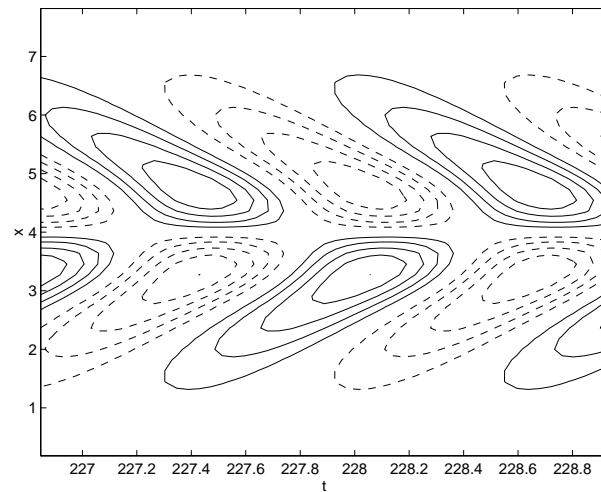


Fig. 3. Butterfly Diagram for Oscillatory Dipole: $\tau = 0.1$, $D = -300$. Contour map of an oscillatory dipole toroidal field $B(x, 0.5, t)$ against x and t . Solid lines are contours of positive magnetic field whilst broken lines denote negative field. The dynamo waves migrate towards the equator.

in Fig. 3. The figure clearly shows the migration of dynamo waves from the pole to equator and the antisymmetric nature of the toroidal field. It can also be easily seen that for this dynamo number the solution is periodic, with a period that is compatible with the linear frequency.

The time-series for $D = -400$ show that as the magnitude of the dynamo number is increased further the periodic dipole solution has lost stability in a secondary Hopf bifurcation to a mixed-mode solution. Fig. 4 clearly shows that both the magnetic and kinetic field energies of solutions are modulated on a longer timescale. Fig. 4c shows that the parity of solutions also undergoes significant fluctuations both on a magnetic cycle frequency and a modulation frequency. This is exactly the type of modulation that has been typically found in dynamo models in the past (e.g. Moss et al. 1990) and was described as Type 1 modulation in the introduction. Here the modulational frequency is of the same order as the beat frequency between the frequency of the linear dipole and quadrupole solutions. In the PDE simulations of Brandenburg et al. (1989), this frequency of modulation is always associated with this ‘beating’. However, in the low order model constructed by Knobloch & Landsberg (1996) it was demonstrated that other modulational frequencies (driven by the choice of nonlinear coefficients) were possible.

However, this type of modulation is not the type observed on the sun, as noted in the introduction. This is made clear on viewing the form of the solutions in the butterfly diagram for the toroidal field shown in Fig. 5. It is clear that the changes in parity arise through a decoupling of the northern and southern hemispheres and the modulation is due to the oscillations in the two hemispheres moving in and out of phase. This can be detected as the relative shifting of the wings of the butterfly diagram. In the sun the two hemispheres appear to remain strongly

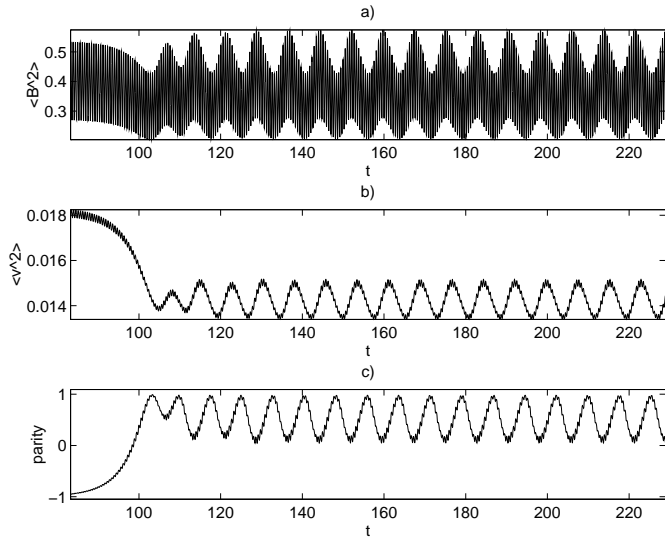


Fig. 4. Quasiperiodic mixed mode: $\tau = 0.1$, $D = -400$. **a** Quasiperiodic magnetic energy. **b** As for **a**, but time series of the average kinetic energy. **c** As for **b**, but time series is of the parity of solutions. Notice that the large changes in magnetic energy are all associated with significant changes in the parity of solutions.

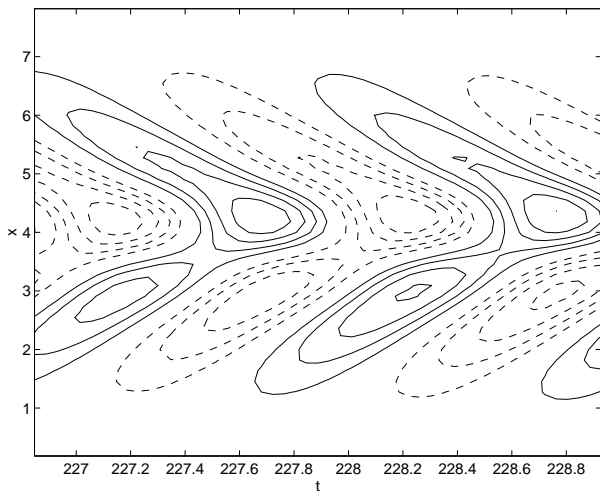


Fig. 5. Butterfly Diagram for Quasiperiodic Mixed Mode: $\tau = 0.1$, $D = -400$. As for Fig. 3, but now the solution is mixed. The hemispheres have moved out of phase and the modulation is due to the changing in phase of solutions. This is not the behaviour observed on the Sun.

coupled and in phase and it is the number of sunspots that is modulated on the longer time-scale.

This branch of quasiperiodic mixed mode solutions ends in a secondary Hopf bifurcation as it collides with the (previously unstable) branch of oscillatory quadrupoles. Again the solutions are periodic as there is no parity modulation. The fact that the solutions have entered the quadrupole subspace shows that, once the dynamo number is sufficiently supercritical, there is no residual preference in the system for remaining at a particular (given) parity. Moreover, although the quadrupoles are found at

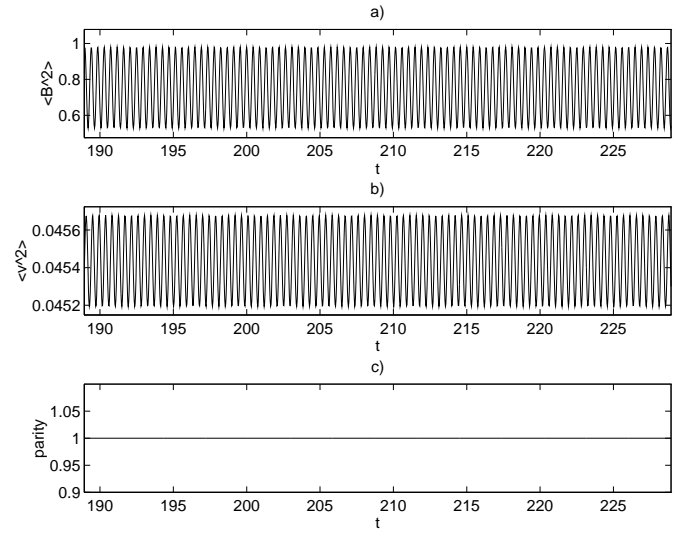


Fig. 6a–c. Weakly modulated quadrupole: $\tau = 0.1$, $D = -700$. **a** Quasiperiodic magnetic energy. **b** As for **a**, but time series of the average kinetic energy. **c** As for **b**, but time series is of the parity of solutions. The magnetic and kinetic energies are very weakly modulated whilst the parity stays at $P = 1$ (quadrupolar).

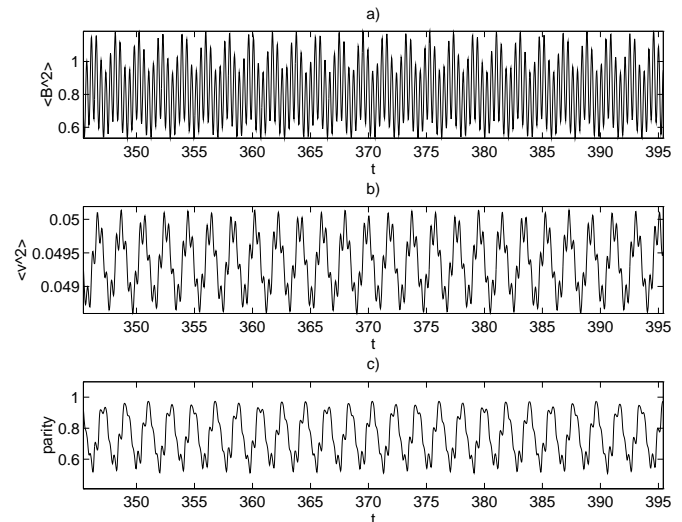


Fig. 7a–c. Strongly modulated mixed-mode: $\tau = 0.1$, $D = -800$. **a** Quasiperiodic magnetic energy. **b** As for **a**, but time series of the average kinetic energy. **c** As for **b**, but time series is of the parity of solutions. The magnetic and kinetic energies are now significantly modulated. Both modulation mechanisms are now in operation and the parity shows significant fluctuations.

larger dynamo numbers than the quasiperiodic mixed modes, their temporal behaviour is much simpler.

The oscillatory quadrupole remains stable until it loses stability in a secondary Hopf bifurcation at a value of D just smaller than $D = -700$. The nature of this secondary Hopf bifurcation is different from the one described earlier. After the secondary Hopf bifurcation solutions are quasiperiodic, but they remain quadrupolar in symmetry as shown in Fig. 6, causing a weak

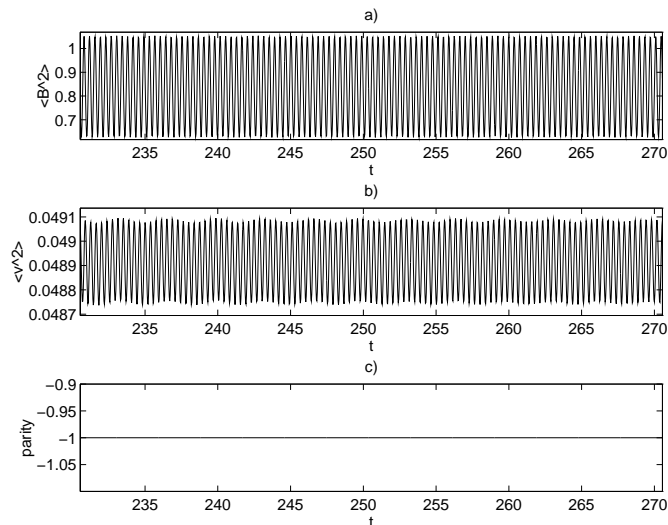


Fig. 8a–c. Modulated dipole: $\tau = 0.1$, $D = -925$. **a** Quasiperiodic magnetic energy. **b** As for **a**, but time series of the average kinetic energy. **c** As for **b**, but time series is of the parity of solutions. The magnetic and kinetic energies are weakly modulated on a timescale controlled by τ but solutions remain dipolar.

version of the Type 2 modulation discussed in the introduction to be observed. (The basic cycle is only *very* weakly modulated in Fig. 6, as the chosen dynamo number is only marginally greater than the bifurcation value.)

Further increase in the value of the dynamo number to $D = -800$ yields solutions that are of mixed parity and are quasiperiodic (as shown in Fig. 7). It appears as though the branch of quasiperiodic quadrupoles has lost stability in a pitchfork bifurcation to the branch of quasiperiodic mixed modes. Significant modulation of the magnetic and kinetic energies can be seen, although again this appears to take place due to the decoupling of the two hemispheres and the subsequent (quasiperiodic) oscillations between states of different symmetries. For this solution both modulation mechanisms are acting, the Type 1 modulation appears to be the stronger of the two although it seems as though the modulation occurs on a timescale selected by the low magnetic Prandtl number (τ) – and hence the Type 2 modulation.

Curiously, this mixed-mode solution appears to lose stability in another pitchfork bifurcation to a purely dipolar solution. The time-series for the magnetic and kinetic energies and parity for $D = -925$ are shown in Fig. 8. It is clear that solutions have reentered the dipole subspace (i.e. that region of phase space where the magnetic energy in the quadrupole mode is identically zero) and, as for the case with $D = -700$, the weak modulation cannot be due in any way to dipole/quadrupole interactions. The modulation must therefore be of Type 2, and must result from the action of the velocity perturbations. Without the parity interactions to amplify it the modulation of the basic cycle is very slight.

However if the magnitude of the dynamo number is increased slightly the Type 2 modulation becomes significantly

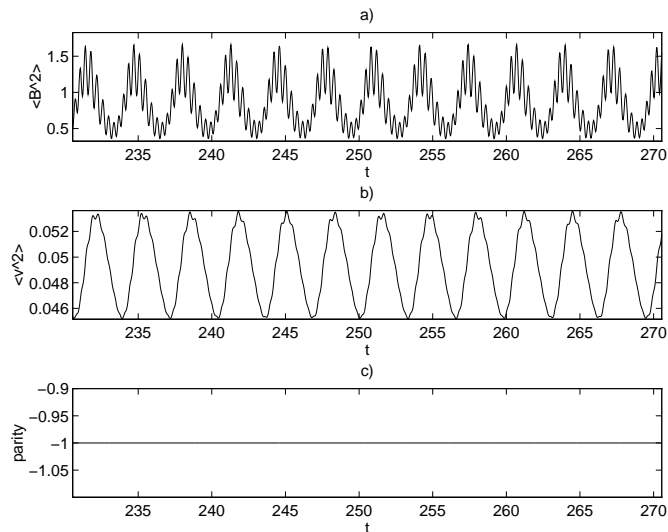


Fig. 9a–c. Strongly Modulated dipole: $\tau = 0.1$, $D = -950$. **a** Quasiperiodic magnetic energy. **b** As for **a**, but time series of the average kinetic energy. **c** As for **b**, but time series is of the parity of solutions. The magnetic and kinetic energies are now significantly modulated.

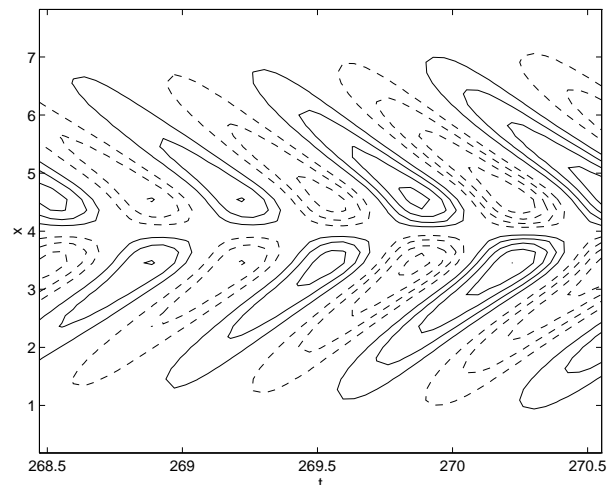


Fig. 10. Butterfly Diagram for Quasiperiodic Dipole: As for Fig. 3 but $\tau = 0.1$, $D = -950$. The dynamo waves migrate towards the equator and it is clear that the basic magnetic cycle is modulated whilst the toroidal field retains its antisymmetry about the equator.

more marked (as shown in Fig. 9). For $D = -950$ the modulation is now large enough to be detected in the butterfly diagram for the toroidal field (Fig. 10). This butterfly diagram makes clear that the modulation is of Type 2. The two hemispheres remain coupled (so that the parity stays dipolar) and the toroidal field is modulated by the velocity perturbations. This behaviour has the same characteristics as that found in the imposed-parity calculations of Tobias (1996a). Solutions remain dipolar as the dynamo number is increased further and the modulation becomes more significant. The magnetic energy now spends a considerable amount of time near a minimum energy state (i.e. near to the invariant manifold $E = 0$).

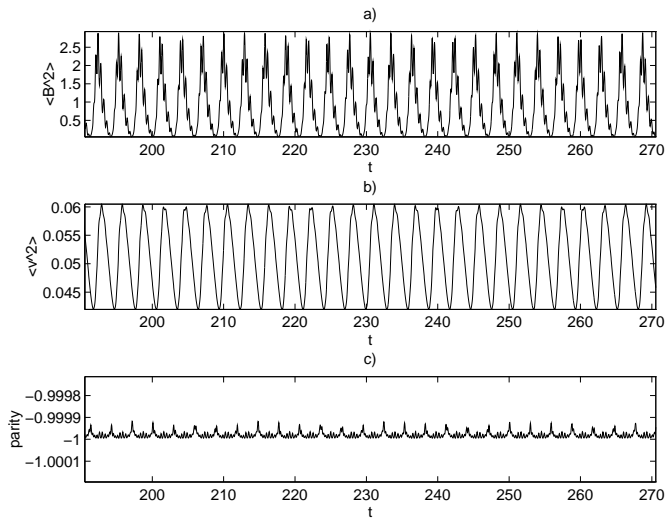


Fig. 11a–c. Strongly Modulated Solution with weak symmetry-breaking: $\tau = 0.1$, $D = -1100$. **a** Magnetic energy **b** As for **a**, but time series of the average kinetic energy. **c** As for **b**, but time series is of the parity of solutions. The magnetic and kinetic energies are significantly modulated and solutions remain largely dipolar. However when the total magnetic energy is very small the solutions show asymmetric tendencies and the parity moves away from $P = -1$.

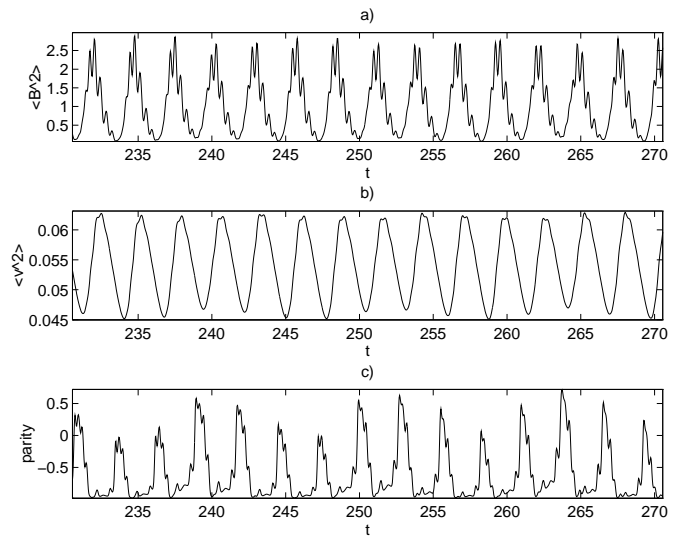


Fig. 13a–c. Strongly Modulated Solution with strong symmetry-breaking: $\tau = 0.1$, $D = -1200$. **a** Chaotically modulated magnetic energy. **b** As for **a**, but time series of the average kinetic energy. **c** As for **a**, but time series is of the parity of solutions. The magnetic and kinetic energies are significantly modulated and solutions are (largely) dipolar except when the field is weak. The modulation is still clearly on a timescale controlled by the magnetic Prandtl number τ . A strong quadrupole component is clearly present when the total energy is small. This is the behaviour observed on the Sun.

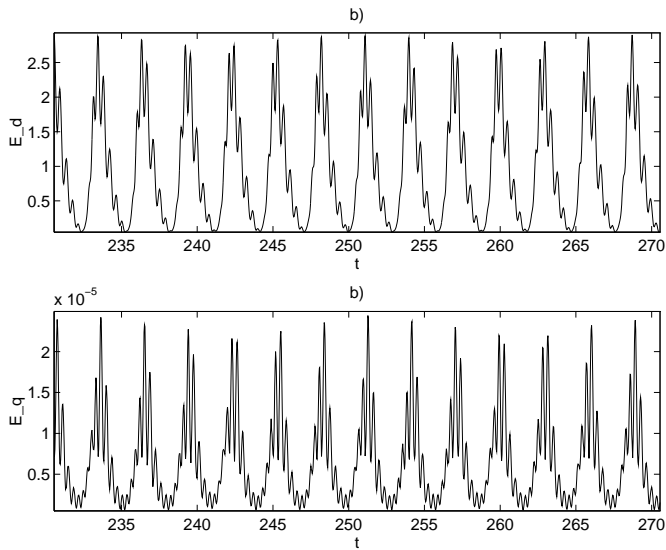


Fig. 12a and b. Comparison of dipole and quadrupole energies: $\tau = 0.1$, $D = -1100$. **a** Dipole energy. **b** Weak quadrupole energy. The quadrupole energy is much smaller than that in the dipole modes and only contributes to the parity when the dipole energy is small (at a minimum of energy).

However now an interesting (and entirely new) transition occurs as D is increased further as shown in Fig. 11. Here the magnetic energy and kinetic energy profiles are similar to those in Fig. 10, but the time-series for the parity in 11c display a different phenomenon. The solutions spend most of the time in (or very close to) the dipole subspace, but, when the field is small and the magnetic energy is low, a (very small) quadrupolar

component of the field can be detected. For $D = -1100$ this effect is very weak (the energy in the quadrupole modes is at most 5×10^{-5} times that in the dipole mode). The energies stored in the dipole and quadrupole modes are shown separately in Fig. 12. Both modes can be seen to be contributing to the mixed mode solution are quasiperiodic or chaotically modulated. It also becomes clear that the energy in the quadrupole is *much* smaller than that in the dipole. Hence the full solution may only display its mixed character when the dipole energy is very low indeed. Consequently the symmetry breaking described here is different in nature from the one discussed earlier.

The quadrupolar component of the mixed mode solution should grow as D moves further away from the critical value for transition to mixed modes. So, for larger dynamo numbers, when the dipole energy is small (i.e. when solutions undergo minima), we expect that there will be occasions when the energy in the quadrupole modes will be comparable (or even larger) than that in the dipole modes. This is indeed the case for $D = -1200$. Here the behaviour most closely resembles that observed on the Sun, as shown in Fig. 13. The total magnetic energy is chaotically modulated on a timescale controlled by τ and the solution stays largely dipolar when the total energy is large. However when the solution enters a minimum the parity moves away from $P = -1$ and the solution displays its mixed nature. The reason for this is shown in Fig. 14. The maximum energy in the quadrupole mode has now grown to an appreciable fraction of the energy in the dipole mode. However, when the dipole energy is large the solution remains close to $P = -1$. and it is

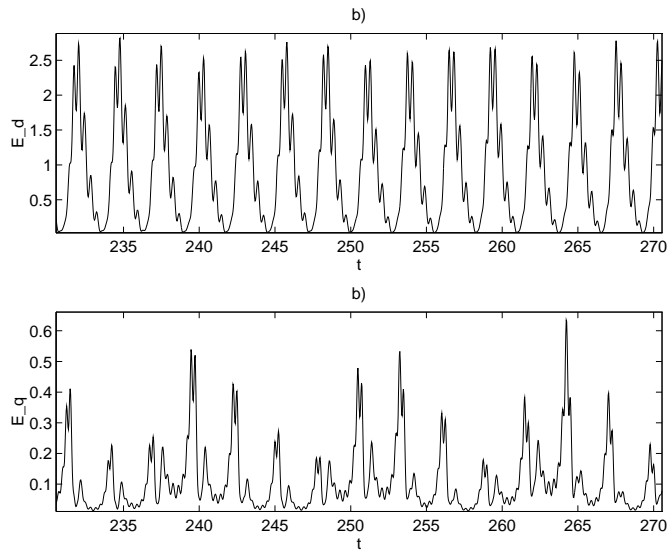


Fig. 14a and b. Comparison of dipole and quadrupole energies: $\tau = 0.1$, $D = -1200$. **a** Chaotically modulated dipole energy. **b** Weak chaotic quadrupole energy. The quadrupole energy has now grown to a significant fraction of the dipole energy. Hence when the dipole energy is small the solutions are completely mixed, is much smaller than that in the dipole modes and only contributes to the parity when the dipole energy is small (at a minimum of energy).

only when the energy in the dipole field enters a minimum that the parity of solutions makes a significant excursion away from $P = -1$. The similarity with the observed behaviour of the Sun extends to the butterfly diagram for the toroidal field (Fig. 15). This butterfly diagram only displays a few magnetic cycles – but it clearly shows the behaviour of the dynamo as it passes through a minimum. The toroidal field is antisymmetric (dipole) as it enters the minimum, but as it emerges it has comparable dipole and quadrupole energies and the field is concentrated in one hemisphere. A couple of cycles after the minimum, dipole symmetry is re-established and the dynamo works ‘normally’ in both hemispheres.

This behaviour continues for larger values of D (with the quadrupole field growing in importance with increasing $|D|$) until the method of solution breaks down due to insufficient numerical resolution.

4. Dependence of solutions on τ

In the last section results were presented for a particular choice of the magnetic Prandtl number $\tau = 0.1$. It is quite clear that this parameter plays an important rôle in the dynamics of the dynamo, controlling both the relative strength of the nonlinearity and the timescale for the response of the velocity perturbations and hence modulation of the magnetic cycle.

Ideally one would like to set the parameters so that the ratio of the magnetic frequency to the modulation/minima frequency is similar to that found for the Sun i.e. so that minima should occur roughly every 10 magnetic (or 20 activity cycles). For the case presented in the previous section where $\tau = 0.1$, the

period of modulation was approximately 5 times longer than the magnetic period. In Tobias (1996a) it is postulated that the ratio of the modulation period to the magnetic period scaled as $\tau^{-\frac{1}{2}}$ in the limit of small τ . In this section an argument that explains this scaling is presented and the dependence of the solutions in the full model on τ is investigated.

From the solutions displayed earlier in this paper and those presented in Tobias (1996a) it is appropriate to hypothesise that the dynamo is acting as a ‘relaxation oscillator’. The basic cycle is modulated by the Lorentz force driving velocity perturbations. The natural timescale for the velocity perturbations to respond to this driving is controlled by the diffusion coefficient (in this case the viscosity ν). Similarly these velocity perturbations create magnetic field on the timescale controlled by the magnetic diffusivity. For these types of coupled relaxation oscillators the overall relaxation timescale is given by

$$t_{\text{relax}} \sim \frac{l^2}{\sqrt{\eta\nu}}.$$

To calculate the modulational timescale T_m , i.e. the relaxation timescale non-dimensionalised in units of the magnetic diffusion time $t_{\text{mag}} \sim l^2/\eta$, it is necessary to calculate

$$T_m = \frac{t_{\text{relax}}}{t_{\text{mag}}} \sim \frac{l^2}{\sqrt{\eta\nu}} \frac{\eta}{l^2} = \sqrt{\frac{\eta}{\nu}} \sim \tau^{-\frac{1}{2}}$$

It would therefore be appropriate to conclude that the correct solar ratio could be achieved by setting $\tau = 0.025$. Unfortunately calculating solutions for this value of the magnetic Prandtl number is beyond the capabilities of the numerical code as noted earlier. It is therefore important to check whether the details of the behaviour of the dynamo change significantly as τ changes, and so the results for $\tau = 0.2$ are reported below (although this case gives results that appear to be less relevant to the behaviour observed on the Sun than those outlined in Sect. 3).

The linear theory presented in the previous section and the appendix is independent of the value of τ , and so for all cases the first mode to become unstable is the oscillatory dipole. As for the $\tau = 0.1$ case, the dipole solution loses stability in a secondary Hopf bifurcation to a quasiperiodic mixed mode solution. This solution displays modulation on a timescale that is similar to the one for Type 1 modulation discussed earlier (see Fig. 16). This timescale therefore seems to be independent of the choice of τ , lending support for the conjecture that it is associated with the Type 1 modulation.

As the dynamo number is increased further, the complicated bifurcation structure can be traced, and is similar to that discussed in Sect. 3. The bifurcations are delayed in comparison with the $\tau = 0.1$ case because the relative strength of the nonlinearity has been altered. For sufficiently large dynamo numbers the model exhibits the Type 2 modulation on a timescale controlled by the magnetic Prandtl number. This effect is seen in Fig. 17 where the timeseries for $D = -1300$ are shown. The solutions are nearly exclusively dipolar (with the parity only moving fractionally away from $P = -1$ when the magnetic

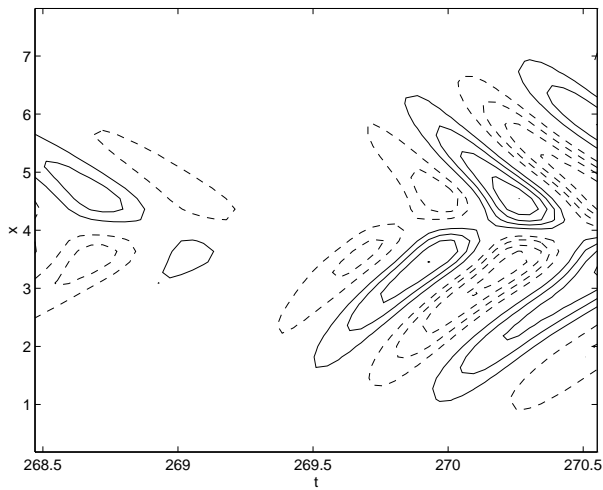


Fig. 15. Butterfly Diagram for the chaotically modulated Mixed Solution: $\tau = 0.1$, $D = -1200$. Contour map of the toroidal field $B(x, 0.5, t)$ against x and t as in Fig. 3. The toroidal field is clearly significantly modulated. Moreover the field is dipolar when strong but, as the solution emerges from a minimum toroidal field can only be found in one (the southern) hemisphere. As the field grows stronger dipole symmetry is reestablished.

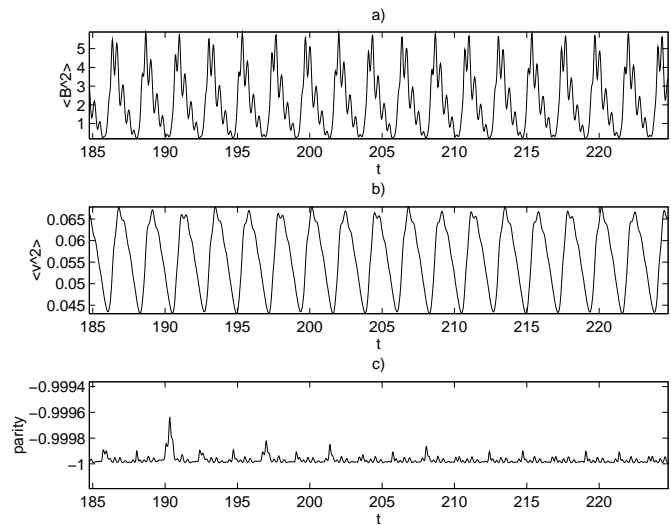


Fig. 17a–c. Strongly Modulated Solution with weak symmetry-breaking: $\tau = 0.2$, $D = -1300$. **a** Magnetic energy **b** As for **a**, but time series of the average kinetic energy. **c** As for **b**, but time series is of the parity of solutions. The behaviour is similar to that shown in Fig. 11. However the modulation frequency has changed by a factor of approximately $\sqrt{2}$. This shows that this modulation is controlled by the value of τ and hence is of Type 2.

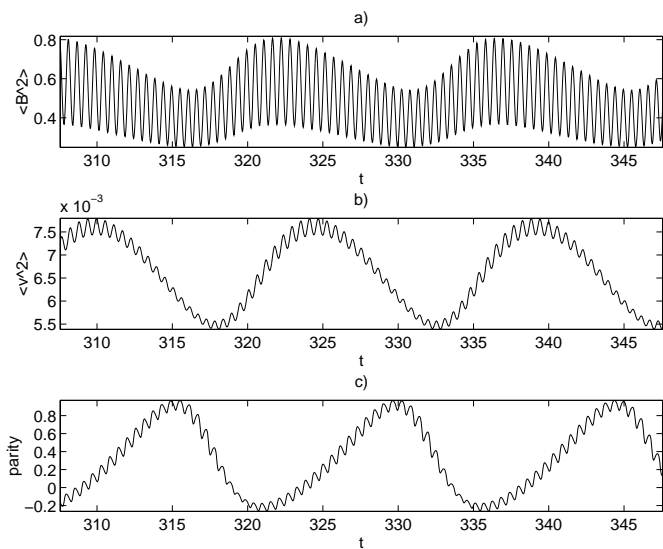


Fig. 16a–c. Quasiperiodic mixed mode: $\tau = 0.2$, $D = -350$ **a** Quasiperiodic magnetic energy **b** As for **a**, but time series of the average kinetic energy. **c** As for **b**, but time series is of the parity of solutions. This solution shows the same type of modulation displayed in Fig 3. The period of this modulation also appears to be independent of the choice of τ .

energy is small) and should be compared with those shown in Fig. 11. For $\tau = 0.2$ the average period of modulation is given by $T_m = 2.2$, whilst for $\tau = 0.1$ the modulation period is approximately given by $T_m = 3.1$. These results are consistent with the scaling $T_m \propto \tau^{-\frac{1}{2}}$ found in the imposed symmetry calculations in Tobias (1996a). A small increase in D from this value leads to solutions exhibiting the ‘solar-type’ behaviour discussed ear-

lier (as shown in Fig. 18) with strong dipolar activity regularly interrupted by asymmetric minima.

The above results would seem to confirm the hypotheses proposed in Sect. 3 that there are two types of modulation, the first of which arises as a result of the interaction between modes of different symmetries on a timescale independent of the magnetic Prandtl number. The second is controlled by the nonlinearity and can arise even when solutions retain dipolar symmetry. The results are consistent with the scaling suggested in Tobias (1996a). Increasing the value of τ delays the onset of the Type 2 modulation because the Malkus-Proctor nonlinearity is weaker for a given dynamo number.

5. Discussion

In this paper I have demonstrated that the modulation and parity changes observed for solar magnetic activity can be explained by the action of an $\alpha\omega$ dynamo with a sufficiently realistic nonlinearity. The results outlined in the previous two sections indicate that modulation of the basic magnetic cycle occurs naturally in the dynamo model due to one of two mechanisms. Neither of these mechanisms acting in isolation is capable of producing results that mimic the observed behaviour of solar activity.

As the dynamo number (and hence rotation rate of the star) is increased in the model, the modulation of the basic cycle initially arises at a secondary Hopf bifurcation because of the ‘parity interaction’ of dipole and quadrupole modes. This parity interaction has been postulated as the mechanism by which the solar cycle is modulated (Sokoloff & Nesme-Ribes 1994, Nesme-Ribes et al. 1996). However the observations of solar

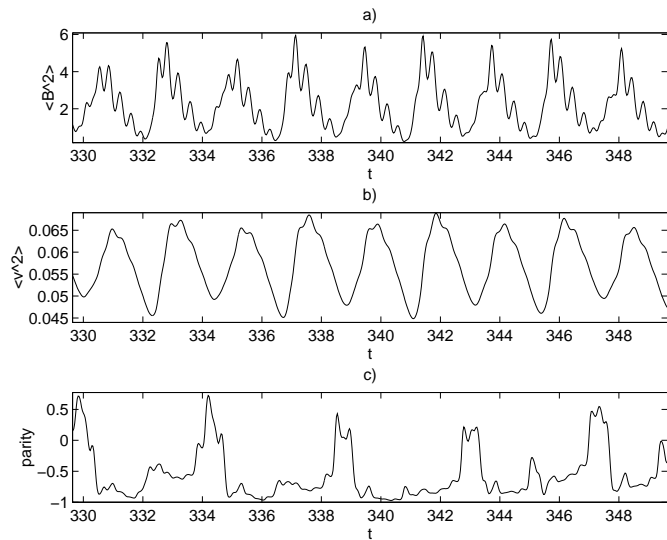


Fig. 18a–c. Strongly Modulated Solution with strong symmetry-breaking: $\tau = 0.2$, $D = -1350$. **a** Chaotically modulated magnetic energy **b** As for **a**, but time series of the average kinetic energy. **c** As for **b**, but time series is of the parity of solutions. The solution again mimics the behaviour of the Sun, with periods of strong energy where the field is largely dipolar interspersed with Minima where the field is mixed and the parity moves away from $P = -1$. Again the period of modulation is controlled by the magnetic Prandtl number τ .

activity would seem to contradict the hypothesis that this phenomenon is of primary importance.

A second mechanism arises naturally from considering the action of the Lorentz force in driving velocity fluctuations. These fluctuations can be observed on the Sun as torsional oscillations (Howard & Labonte 1980, Ulrich et al. 1988). If the natural timescale for the response of the turbulent plasma to the magnetic driving is much longer than the period for the magnetic field, this nonlinearity may lead to chaotic modulation on the long timescale even when the symmetry of solutions is held fixed. The consequences of including a time-lag between the driving and response in a dynamo system were originally investigated by Yoshimura (1975).

When both types of modulation are included in the model the dynamo system initially (for weak fields) prefers to undergo the parity interactions found in many previous dynamo models. As the dynamo number is increased, and the field becomes stronger, weakly modulated solutions of dipole symmetry are preferred. The modulation, resulting from the inclusion of the Malkus-Proctor effect, becomes significant as the dynamo becomes increasingly supercritical. Now solutions display long periods of significantly reduced activity (minima) where the energy in the dipole field is extremely small. During these periods the solutions may, unsurprisingly, adopt the mixed symmetry displayed by the earlier weak-field solutions. Dipole symmetry is only restored when the total magnetic energy is large enough. Strikingly, the butterfly diagram for the toroidal field closely mimics the behaviour of solar activity from the Maunder minimum onwards. As solutions emerge from a minimum, toroidal field appears in only one hemisphere; but when the dynamo is

reestablished the dipole symmetry is again strongly preferred. In this way the symmetry-breaking can be seen to be of secondary importance to the Malkus-Proctor mechanism as the asymmetry only appears when the toroidal field is weak.

Integrations for larger values of the magnetic Prandtl number ($\tau = 0.2$) demonstrate that the conclusions derived from the results for $\tau = 0.1$ are reasonably robust. Again, as D is increased, the initial modulation is due to parity interactions, and Malkus-Proctor type modulation is found as solutions become more supercritical. As in the imposed-symmetry calculation, the results are consistent with the scaling $T_m \propto \tau^{-\frac{1}{2}}$, where T_m is the average period of modulation for quasiperiodic and chaotic solutions (although it is dangerous to extrapolate too much into a scaling law derived from only two parameter values). However, for this larger value of τ the Type 2 modulation is delayed to larger dynamo numbers. This suggests that *decreasing* τ may lead to *both* types of modulation acting strongly for lower dynamo numbers and hence to a different type of behaviour for weak-field solutions. This shift to the coexistence of both types of modulation may well be offset by the inclusion of a secondary nonlinearity (e.g. α -quenching) that could limit the size of the magnetic fields in the overshoot region. Indeed if the α -effect is strongly quenched in the convection zone (as suggested by the recent numerical results of Cattaneo & Hughes 1996) then the strong field must be confined strongly to the overshoot region so as to enable the helical turbulence to generate poloidal field in the convection zone. It is difficult to comprehensively investigate effects such as these (requiring the exploration of large parameter regimes) in this PDE model or even to successfully deduce the nature of all the bifurcations for a limited parameter regime. For this reason a low order system that includes both the types of modulation discussed here is currently being investigated.

It is also interesting to speculate what this set of results implies for the theory of generation of magnetic fields in other stars. Observations of lower main sequence stars show that the magnetic behaviour of the stars changes as the rotation rate (and hence rotational moment) is increased. Recent observations (Baliunas et al. 1996) suggest that as the rotation rate is increased the typical behaviour of the star changes from being periodic to doubly-periodic and finally chaotic (with many stars undergoing minima). This paper may give a better understanding of the transition from periodic to doubly-periodic behaviour in these stars. The results indicate that for very active stars both modulation mechanisms may be important and magnetic activity will both undergo periods of reduced activity and be asymmetric. However for stars that rotate more slowly and have weaker magnetic fields modulation may simply be due to the interaction between dipole and quadrupole modes. Moreover for stars with deep convective envelopes and weak differential rotation, so that the field is generated throughout the convection zone, the Malkus-Proctor effect will be of lesser importance. Any modulation found is therefore more likely to be due to the changes in the parity of solutions. The results suggest that the Sun's dipolar behaviour is not necessarily typical

and that magnetic fields of quadrupolar or mixed symmetries may be found in other stars.

Acknowledgements. I am grateful to Nigel Weiss for his helpful suggestions and to Nic Brummell, Marc DeRosa, John Hart, Keith Julien, Alastair Rucklidge, Manfred Schüssler and Ed Spiegel for illuminating discussion. I would like to thank Trinity College, Cambridge for a research fellowship. The work was completed under NASA SPTP grant NAG5-2256 whilst a research associate at JILA.

Appendix A

The linear solutions are calculated by expanding the toroidal and poloidal fields in Fourier series – the velocity perturbations v may be set to zero for the linear problem. It is not apparent a priori whether the onset of dynamo action occurs at a stationary or oscillatory bifurcation and so both cases must be considered. On contemplating the boundary conditions it is clear that we should proceed by expanding both B and A in Fourier sine series. We therefore set

$$A = \sum_{j=1}^m (a_j^s(z) \sin \omega t + a_j^c(z) \cos \omega t) \sin\left(\frac{j\pi x}{2L}\right) e^{\lambda t},$$

$$B = \sum_{j=1}^m (b_j^s(z) \sin \omega t + b_j^c(z) \cos \omega t) \sin\left(\frac{j\pi x}{2L}\right) e^{\lambda t}, \quad (A1)$$

where m is the number of modes in the Galerkin expansion. Here m is chosen to be 32 – large enough so that consistent, accurate results are achieved. It is clear from the expansions in equation (A1) that the solutions grow (decay) exponentially with growth-rate (decay-rate) λ and oscillate with frequency ω . Hence if the bifurcation to dynamo action is stationary ω will be zero.

Equations for $a_j^s(z)$, $a_j^c(z)$, $b_j^s(z)$ and $b_j^c(z)$ are now derived by substituting expansions (A1) into equation (3) and using simple trigonometric identities to obtain

$$a_j''^s(z) - \left(\frac{\pi j}{2L}\right) a_j^s(z) + \omega a_j^c(z) - \lambda a_j^s(z) + \frac{f(z)}{2} (b_{j-1}^s(z) + b_{j+1}^s(z)) = 0,$$

$$a_j''^c(z) - \left(\frac{\pi j}{2L}\right) a_j^c(z) - \omega a_j^s(z) - \lambda a_j^c(z) + \frac{f(z)}{2} (b_{j-1}^c(z) + b_{j+1}^c(z)) = 0,$$

$$b_j''^s(z) - \left(\frac{\pi j}{2L}\right) b_j^s(z) + \omega b_j^c(z) - \lambda b_j^s(z) + \frac{D\pi u'(z)}{4L} ((j-1)a_{j-1}^s(z) - (j+1)a_{j+1}^s(z)) - \frac{D\pi u(z)}{4L} (a'_{j-1}^s(z) + a'_{j+1}^s(z)) = 0,$$

$$b_j''^c(z) - \left(\frac{\pi j}{2L}\right) b_j^c(z) - \omega b_j^s(z) - \lambda b_j^c(z) + \frac{D\pi u'(z)}{4L} ((j-1)a_{j-1}^c(z) - (j+1)a_{j+1}^c(z)) - \frac{D\pi u(z)}{4L} (a'_{j-1}^c(z) + a'_{j+1}^c(z)) = 0,$$

for $j = 1, m$, where b_j, a_j are zero for $j < 1, j > m$ constitute a two-point boundary eigenvalue problem. This boundary value problem can be solved numerically using the Newton-Raphson-Kantorovitch routine NRK.

As usual, studying the symmetries of the system of equations is a useful procedure. As noted in the main text the eigenfunctions that bifurcate from the trivial ($A = B = 0$) state must be of either pure dipole or pure quadrupole parity. As pointed out by Jennings (1991), a field of pure dipole parity is restricted to odd a_j^s, a_j^c and even b_j^s, b_j^c , while a pure quadrupole has even a_j^s, a_j^c and odd b_j^s, b_j^c . Hence to obtain the initial bifurcation (to either dipole or quadrupole state), only half the number of modes need to be considered.

References

- Baliunas S.L., Sokoloff D., Soon W. et al., in preparation
 Beer J., Raisbeck G.M., Yiou F., 1991, in: *The Sun In Time* eds. C.P. Sonett, M.S. Giampapa, M.S. Matthews, University of Arizona Press, Tucson, p. 343
 Brandenburg A., Krause F., Meinel R. et al., 1989, *A&A* 213, 411
 Cattaneo F., Hughes D.W., 1996, *Phys. Rev. E* 54, R4532
 Eddy J. 1976, *Science* 192, 1189
 Gough D.O., Moore D.R., Spiegel E.A., Weiss N.O., 1976, *ApJ* 206, 536
 Howard R., Labonte B.J., 1980, *ApJ* 239, L33
 Hoyt D.V., Schatten K.H., 1995 *Solar Physics* 160, 379
 Jennings R.L., 1991, *GAFD*, 57, 147
 Jennings R.L., Weiss N.O., 1991 *MNRAS* 252, 249
 Kitchatinov L.L., Rüdiger G., Küker M., 1994, *A&A* 292, 125
 Knobloch E., Landsberg A.S., 1996, *MNRAS* 278, 294
 Malkus W.V.R., Proctor M.R.E., 1975, *JFM* 67, 417
 Moss D., Tuominen I., Brandenburg A., 1990, *A&A*, 228, 284
 Nesme-Ribes E., Baliunas S.L., Sokoloff D., 1996, *Scientific American*, 275, 46
 Parker E.N., 1993, *ApJ* 408, 707
 Platt N., Spiegel E.A., Tresser C., 1994, *GAFD* 73, 147
 Ribes J.C., Nesme-Ribes E., 1993, *A&A* 276, 549
 Sokoloff D., Nesme-Ribes E., 1994, *A&A* 288, 293
 Stuiver M., Grootes P.M., Braziunas T.F., 1995, *Quaternary Research*, 44, 341
 Stix M., 1991, *GAFD*, 62, 211
 Thompson M.J., Toomre J., Anderson E.R. et al., 1996, *Science* 272, 1300
 Tobias S.M., 1996a, *A&A*, 307, L21
 Tobias S.M., 1996b, *ApJ*, 467, 870
 Tobias S.M., Weiss N.O., Kirk V., 1995, *MNRAS* 273, 1150
 Ulrich R.K., Boyden J.E., Webster L. et al., 1988, *Solar Phys* 117, 291
 Watari S., 1996, *Solar Physics* 163, 259
 Weiss N.O., 1994, in: *Lectures in solar and planetary dynamos*, eds. M.R.E. Proctor, A.D. Gilbert, Cambridge University Press, Cambridge, p. 59
 Weiss N.O., Cattaneo, F., Jones, C.A., 1984, *GAFD* 30, 305
 Yoshimura H., 1975, *ApJSS* 29, 467